Comparative Study on 3D Modelling of Breast Cancer Using Nir-Fdot in Comsol

Soorya Peter
Christ University
Christ University,Banglore,Karnataka,India 560029
sooryapeter@gmail.com

Abstract: Fluorescence Diffuse Optical Tomography (FDOT) uses Near Infra-red (NIR) light to monitor physiological changes in internal organs. In this paper a comparative study on the 3d modelling of breast cancer using NIR-FDOT is discussed. The forward model and the reconstruction are simulated using COMSOL. The forward problem of DOT, is described by the Radiative Transfer Equation used with diffusion approximation .This equation is represented in the form of Helmholtz Equation in COMSOL Multiphysics. A mesh model of a phantom (with optical properties of a human breast) is created and the flux intensity values are modeled using FEM with the coefficients (quantum yield, molar extinction coefficient etc.) obtained from the in-vitro studies. Where the values of the quantum yield and molar extinction coefficient obtained for an estrogen conjugate fluorescent dye are 0.144 and 6.25e5 M-1cm-1 respectively. Both the excitation (750nm) and emission (783nm) equations are inverted using Levenberg-Marquardt method with Tikhonov minimization of measurement. COMSOL simulations were carried out to obtain the fluence rate for multiple fluorescent inclusions.

Keywords : NIR-FDOT , Helmholtz equation , inverse problem, fluence rate.

1. Introduction

Light imaging techniques in the near-infrared (NIR) window benefit from low tissue absorption. Since photons can propagate over several centimetres within biological tissues in NIR wavelength, NIR photons can be used to explore the inner tissue structure. Recently, the development of NIR fluorescent markers has led to a new imaging technique, namely fluorescence diffuse optical tomography (FDOT), able to determine the 3D local concentrations of fluorescent agents. Such markers have been increasingly studied in the last years[5]. Some of them have been designed to fix on specific proteins then behaving as molecular probes. Others called activable become fluorescent only in the vicinity of a given protein .Near-infrared tissue spectroscopy and imaging offer many promising non-invasive medical applications such as the localization of tumors and the monitoring of physiological parameters such as haemoglobin saturation and glucose concentration. Traditionally, both the high sensitivity and the selectivity of fluorescence spectroscopy have made it an attractive tool for detecting traces of specific chemical compounds. Fluorescence offers enhanced sensitivity to NIR spectroscopy and enhanced image contrast. [6]

Fluorescence is a spectrochemical method of analysis where the molecules of the analyte are excited by irradiation at a certain wavelength and emit radiation of a different wavelength. The emission spectrum provides information for both qualitative and quantitative analysis. Considering a set of external light excitations and a resulting set of external fluorescent light detections, a tomographic scheme can be applied to a medium injected with fluorescence markers to recover local concentration in fluorescent markers. This reconstruction implies the use and the inversion of an appropriate model accounting for both the photon propagation and the fluorescence phenomena. In this paper the fluorescence phenomena (used in breast cancer detection) is simulated using comsol multiphysics and corresponding fluence rate observed.

2.Theory

2.1 Fluorescence parameters of interest and fluorescence phenomena in tissue

A spectroscopist views tissue as a collection of chromophores – constituents which interact with light in some manner.[4] For the purpose of fluorescence spectroscopy three types of interaction with light are important: absorption, scattering and fluorescence. Chromophores are hence classified as absorbers, scatterers and/or fluorophores. Absorbers are chromophores that do not fluoresce , fluorophore to mean chromophores that absorb and re-radiate some absorbed light in the form of fluorescence. Absorbers and fluorophores can both elastically scatter light. Each chromophore can be characterised by a set of optical properties: the

wavelength dependent absorption coefficient , $\mu_{ak}(\lambda)$, scattering coefficient , $\mu_{sk}(\lambda)$, anisotropy factor , $g_k(\lambda)$, and quantum yield , $\phi_k(\lambda i,\lambda j)$, which is dependent on both excitation(λi) and emission(λj) wavelength. The propagation of light in the tissue sample is generally described in terms of tissue optical properties: $\mu_{ak}(\lambda)$, $\mu_{sk}(\lambda)$, $g_k(\lambda)$. Here, the absorption and scattering coefficients represent the total absorption and scattering coefficients of the sample and can be regarded as the sum of absorption and scattering coefficients of all tissue chromophores. The anisotropy factor ,g, represents the average cosine of the scattering angle of the tissue as a whole.

The fluorescent signal is affected by multiple scattering at both the excitation and the emission wavelengths.[1] In Fig. 1.1, a diagram shows that the excitation light at wavelength λ is an isotropic point source at **rs**, and that the fluorescent light at wavelength λ*e*, which is emitted from a fluorophore at **r**', is collected at point **r**. The absorption coefficient, the reduced scattering coefficient, and the refractive index of the background medium at λ are denoted, respectively, as μ*a*, μ'*s*, and *n*, and at λ*e* as μ*ae*, μ'*se*, and *ne*.[1]

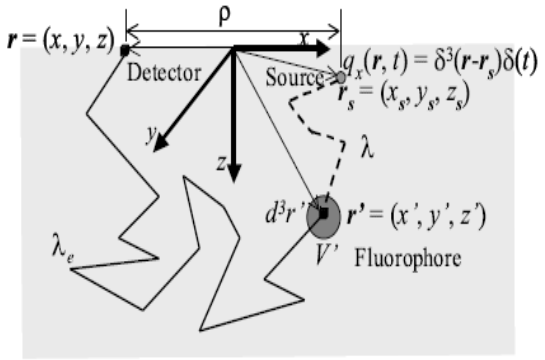

Fig 1.2 : Light propogation in tissue with fluorophore

2.2 Light Propogation

The NIR light propagation within a turbid media such as biological tissues has been successfully modeled by the diffusion theory. Indeed, the photons density ϕ (**r**, *t*) at position **r** and time *t*, in a medium wherein the scattering probability is much larger than the absorption, satisfies the photon diffusion equation. In particular, regarding a light pulse emitted at position **r**' and time zero into an optically homogeneous medium, it can be stated that[5]:

$$\frac{1}{v}\frac{\partial}{\partial t}\phi(\mathbf{r},t) - D\nabla^2\phi(\mathbf{r},t) + \mu_a\phi(\mathbf{r},t) = S\delta(\mathbf{r}-\mathbf{r}',t)$$

Where $v = c/n$ (cm.ns-1) is the speed of light in the medium of refractive index *n*. δ represents the Dirac function. *S* is the intensity of the input signal (W.cm-3). $D = 1/3\mu_s'$(cm) is the diffusion constant. μ_s' (cm-1) is known as the reduced scattering coefficient and μa is the absorption coefficient .

2.3 Fluorescence

The fluorescence signal *Ufl*, measured in FDOT, results from a three-stage process. First, light emitted at the wavelength λ*em* propagates through the medium from the excitation point to a fluorescent marker. Second, the fluorescent marker absorbs excitation light and reemits fluorescence light at the wavelength λ*ex*<λ*em*. Third, the fluorescence light propagates through the medium from the fluorescence marker to the detector. This process can be modeled in the time domain as[5]

$$U_{fl}(\mathbf{r}_s,\mathbf{r}_d,t) = A\int\phi_{ex}(\mathbf{r}_s,\mathbf{r},t)*_t F(\mathbf{r},t)*_t \phi_{em}(\mathbf{r},\mathbf{r}_d,t)d^3r$$

where $\mathbf{r}_s$ and $\mathbf{r}_d$ are respectively the positions of the excitation and detection points. *A* is a constant taking into account experimental parameters (such as transmission of filters, neutral densities, detectors quantum efficiencies, etc). The integration is performed all over the diffusing medium and $*t$ denotes the time convolution operator. The subscript *ex* and *em* indicates whether the photon densities ϕ are to be considered at the excitation wavelength λ*ex* or emission wavelength λ*em*. The pulse response *F*(**r**, *t*) of the fluorescent marker at position **r** is classically modeled by the exponential decay characterized by the lifetime τ(ns)[5] :

$$F(\mathbf{r},t) = \eta c(\mathbf{r})\frac{e^{-t/\tau}}{\tau}$$

c(**r**)(μM) is the marker concentration at position **r** and η(-) is the quantum yield of fluorescence.

2.4 Forward Problem

Laser beam interaction (both excitation and re-emission) with tissue in NIR window can be modeled using Standard Diffusion Approximation (SDA) or P1 approximation of Radiative Transport Equation (RTE). The excitation and emission of fluorescent dye can be modeled as two coupled SDA equations. In frequency domain the diffusion equation become elliptical and can be expressed as[7]

$$-\nabla.(D_x\nabla\phi_x(r)) + \left[\mu_{axi} + \mu_{axf} + \frac{i\omega}{c}\right]\phi_x(r) = -\Theta_s\delta(r-r_s) \quad (1a)$$

$$-\nabla.(D_m\nabla\phi_m(r)) + \left[\mu_{ami} + \frac{i\omega}{c}\right]\phi_m(r) = -\frac{\phi_x(r)\eta\mu_{axf}}{1-i\omega\tau} \quad (1b)$$

$r \in \Omega$

Where

$$D_x = \frac{1}{3(\mu_{axi} + \mu_{axf} + \mu'_{sx})}$$

$$D_m = \frac{1}{3(\mu_{ami} + \mu'_{sm})}$$

$\theta_s\delta(r\text{-}r_s)$ is the excitation light source of power θ_s and one diffusion length away from boundary. $\Phi_{x,m}$ is the photon fluence.η is fluorescent quantum efficiency and ζ is fluorescent life time. The subscript *x* and *m* denote the excitation and emission light wavelengths. Subscript *i* in optical property indicates internal tissue properties and *f* indicates properties introduced due to fluorescent dye injection μa,μs' and are absorption and reduced scattering coefficient respectively.

Subjected to Robin boundary conditions[7]

$$\mathbf{n}.[2A_x D_x \nabla\phi_x(r)] + \phi_x(r) = 0 \quad \forall r \in \partial\Omega \quad (2a)$$

$$\mathbf{n}.[2A_m D_m \nabla\phi_m(r)] + \phi_m(r) = 0 \quad \forall r \in \partial\Omega \quad (2b)$$

Where equation 1a and 1b models excitation light and generation and propagation of fluorescence emitted light respectively, **n** is the normal vector to the boundary , is the critical angle, A is refractive index mismatch at the boundary given by

$$A = \frac{2/(1-R_0) - 1 + |\cos(\theta_c)|^3}{1 + |\cos(\theta_c)|^2}$$

where

$$R_0 = (n_1 / n_{AIR} - 1)^2 / (n_1 / n_{AIR} + 1)^2$$

Where n_1 is the refractive index of domain and n_{AIR} is the refractive index of air.

2.5 Inverse Problem

The goal of inverse problem is to recover optical properties at each node point within the domain using measurements of light fluence at the boundary[2].The inversion can be obtained by using a modified Tikhonov minimization.

$$\chi^2 = \min_{\mu} \left\{ \sum_{i=1}^{M} (\phi_i^M - \phi_i^C)^2 \right\}$$

Where M is total number of measurements obtained, ϕ^m is the measured fluence at the tissue surface and ϕ^c is the calculated fluence using the forward solver. Minimization with respect to μ is obtained by equating the first derivative to zero and ignoring higher order terms

$$\left(\frac{\partial\phi^C}{\partial\mu} \right)^2 (\phi^M - \phi^C) = 0$$

$\frac{\partial\phi^C}{\partial\mu}$ is called Jacobian matrix J.

Using linear approximation of the problem and solving it in an iterative scheme gives [2]

$$(J^T J + \lambda I)\partial\mu = J^T \partial\phi$$

Where λ is the Tikhonov regularization parameter ,δμ is the update of optical properties and δϕ is the measurement misfit at current iteration . Modifying the above equation using Levenberg-Marquardt (LM) procedure gives[2]

$$\partial\mu = (J^T J + \bar{\lambda} I)^{-1} J^T \partial\phi$$

The optical properties are updated using this equation.

For a frequency domain system both the amplitude and phase values are available, so the Jacobian contain sub matrices of log magnitude and phase.

$$\frac{\partial \ln I_i}{\partial D_j}, \frac{\partial \ln I_i}{\partial \mu_j}, \frac{\partial \theta_i}{\partial D_j}, \frac{\partial \theta_i}{\partial \mu_j}$$

3.Use of Comsol Multiphysics

In this paper the forward model and the reconstruction are simulated using COMSOL. The forward problem of DOT, which involves obtaining of the radiance values of light at the boundary of the specimen (with known μa and μs values) after irradiating it with NIR radiation, can be described by the Radiative Transfer Equation used with diffusion approximation .This equation is represented in the form of an Helmholtz Equation in COMSOL Multiphysics.

$$\nabla(-c\nabla u) + au = f$$

With Parameters,

$$u = \phi$$

$$c = D = \frac{1}{3(\mu_a + \mu_s')}$$

$$a = \mu_a$$

$$f = S$$

To model fluorescence in Multiphysics, one first solves the diffusion equation (a Helmholtz equation) for the excitation light, which will act as the source term for the fluorescence. The fluorescence light propagation is then modeled by adding another Helmholtz equation and solving for the fluence rate.The "emission" Helmholtz equation is given another set of optical properties

since the wavelength is different as compared to the excitation light. The following equations in steady-state represent this in a formal way:

$$\Phi_x(r) - \nabla D_x(r)\nabla\Phi_x(r) + \mu_{ax}\Phi_x(r) = S_x(r)$$

$$\Phi_m(r) - \nabla D_m(r)\nabla\Phi_m(r) + \mu_{am}\Phi_m(r) = \mu_{af}\gamma_m\Phi_x(r)$$

4.Results And Discussions

A 3d model of a phantom with optical properties similar to that of a human breast is simulated using COMSOL. 20 point sources emitting NIR radiation at 750nm are placed around the phantom which provides the excitation flux.

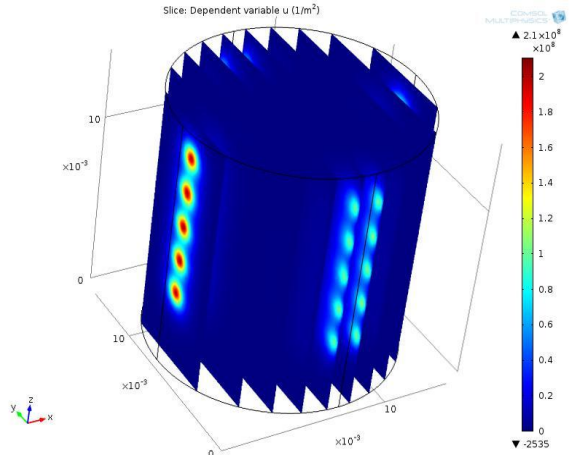

Fig 4.1: Simulated model of a the phantom surrounded with 20 sources emitting NIR radiation at 750nm, as viewed in the yz plane,using 10 slices.

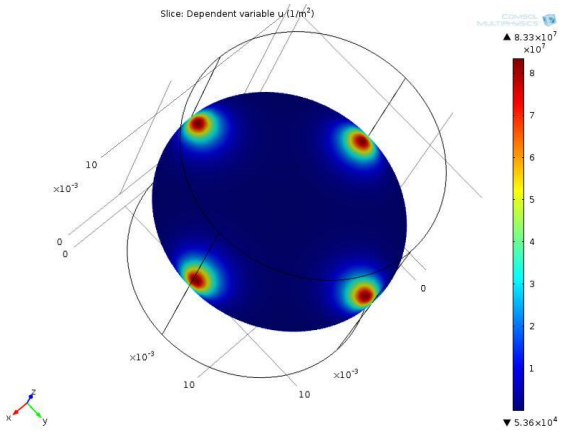

Fig 4.2: Simulated model of a the phantom surrounded with 20 sources emitting NIR radiation at 750nm, as viewed in the xy plane,using 1 slice.

The optical properties of the phantom(breast tissue) used in the computational model were[3]:
Absorption coefficient μ_a = 0.036cm^{-1}
Scattering coefficient μ_s = 10.20cm^{-1}
Diffusion coefficient D = 0.0326cm
These properties are at the excitation wavelength of 750nm.

A 3d mesh model was generated on the entire structure and is refined in the regions of interest like the point sources and the inhomogenity because the mesh defines the accuracy of the solution. If a too coarse mesh is used the diffusion equation solution is most likely erroneous due to discretization errors. On the other hand going for the finest resolution of the mesh directly will render a large number of mesh elements that many computers can't store in memory.

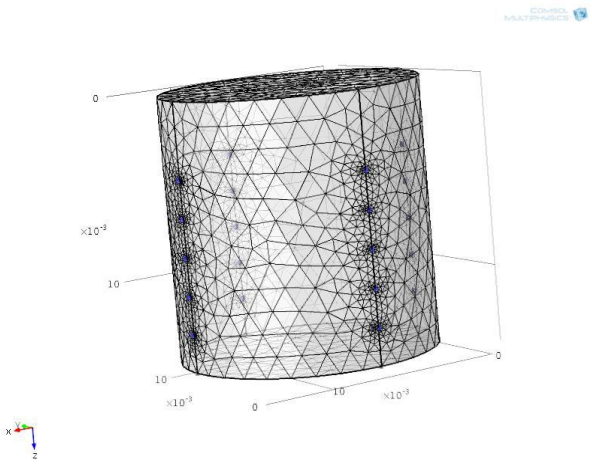

Fig 4.3: 3d Mesh model of the phantom and the point sources. The meshing around the point sources here are more refined.

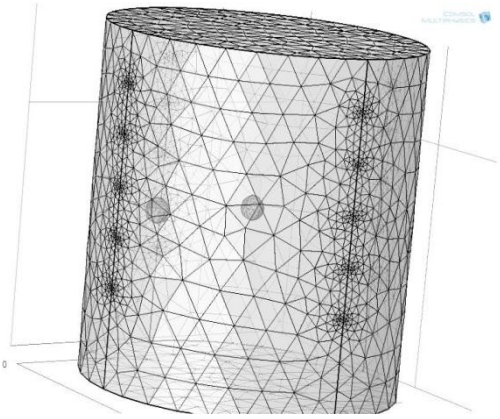

Fig 4.4 : 3d Mesh model of the phantom ,the point sources and the two added anomalies. The meshing around the point sources and inhomogenity are more refined.

The photon fluence rate, represented here as u, is the total amount of power density available at a particular point. The measurement of this fluence

rate is the first task in tissue optics. Inorder to obtain the inverse model to detect the inhomogenity, the fluence rate has to be obtained. Hence the fluence measurement is of utmost importance.

After simulating the phantom along with the sources, the fluence rate was plotted with respect to arc length and reverse arc length. The dimension of the cylinder used for the simulation were:
Radius = 7cm
Height = 14cm

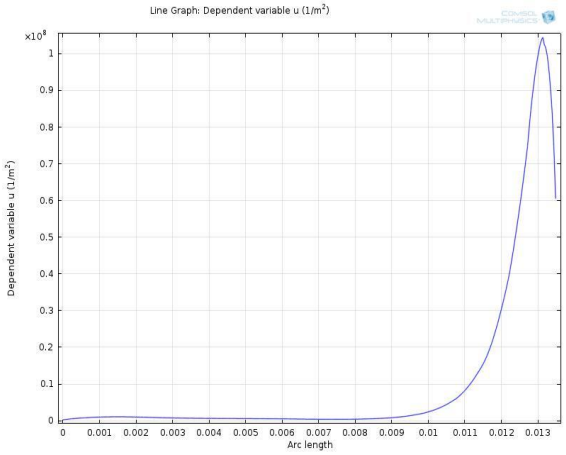

Fig 4.5 : figure shows the plot of fluence rate of sources measured from x=14. The fluence rate is maximum near the sources and diminishes with the increase in the distance from the source.

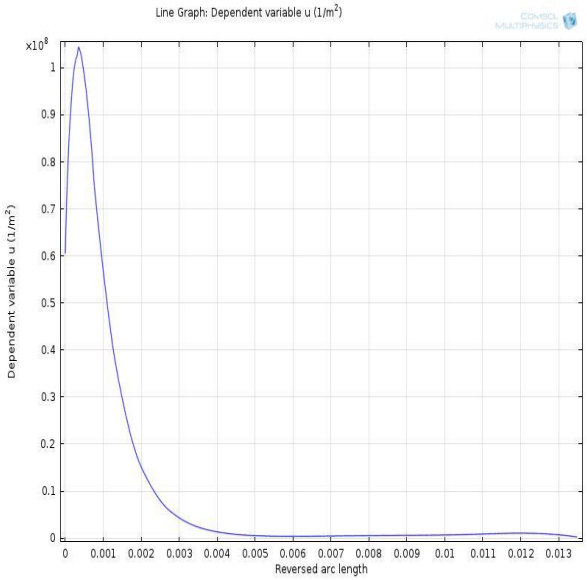

Fig 4.6 : figure shows the plot of fluence rate of sources measured from x=0. The fluence rate is maximum near the sources and diminishes with the increase in the distance from the source.

To the phantom an anomaly was added which is a fluorophore. It absorbs the excitation wavelength supplied and emitts radiation at a different wavelength, here 783nm.

The fluorescence light that is to be modeled is emitted at another wavelength than the excitation light. Hence the optical properties are different.

The optical properties of the anomaly used in the computational model were[3]:
Absorption coefficient $\mu_a = 0.0412cm^{-1}$
Scattering coefficient $\mu_s = 9.09cm^{-1}$
Diffusion coefficient D = 0.0366cm
These properties are at the emission wavelength of 783nm.

FDOT helps in the identification of the local concentration of certain fluorescent agents.The fluorophore absorbed the excitation light and re-emitted at emission wavelength.This is simulated using COMSOL.

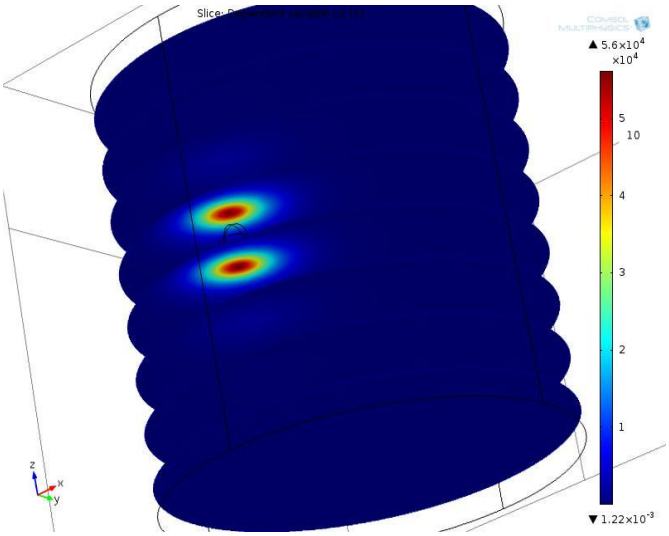

Fig 4.7 : The sphere here represents the flurophore(anomaly) that was added. It absorbed the source radiation and re-emitted at a different wavelength. 8 slices were used and the simulated model here is in the xy plane.

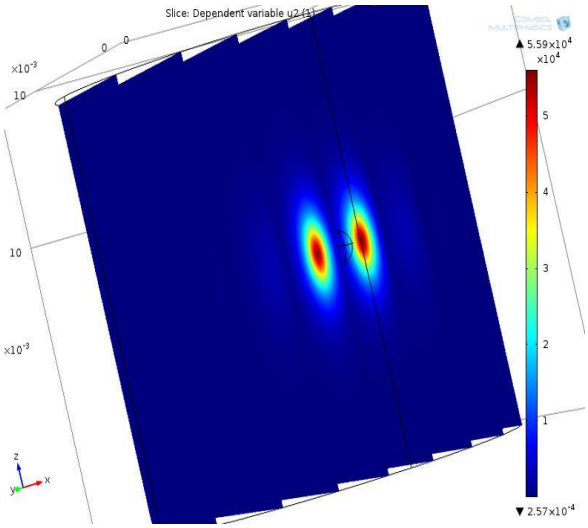

Fig 4.8: the simulated model here is in the yz plane.

This source term for the fluorophore is “muaf*u” where u is the excitation light fluence rate in the cylinder coming from the sources.

The fluence rate given out by the fluorophore is at a different wavelength and detection of this fluence value can indicate the prescence of a particular compound of interest.

The fluence rate with respect to the thickness of the phantom (arc length) is then plotted.

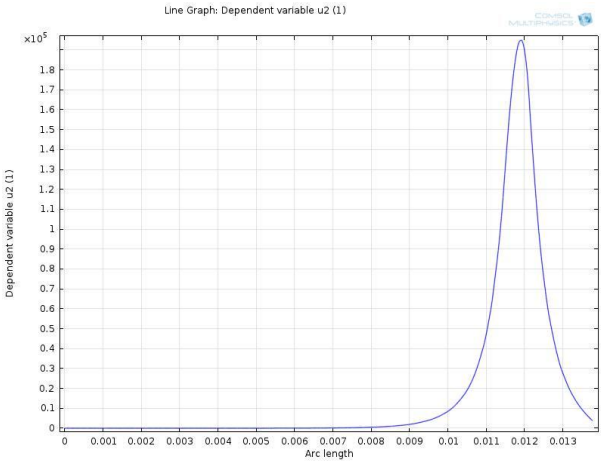

Fig 4.9: The figure shows the plot of the emission fluence rate(u2) with respect to the phantom thickness.

In the above figure the fluence rate is maximun near the fluorescent anomaly and diminishes with distance. Since the mesh is refined at the position of the inhomogenity the fluence values can be obtained from those nodes.

Another fluroscent inclusion is again added to the phantom and the fluorescence of both the inclusions are simulated.

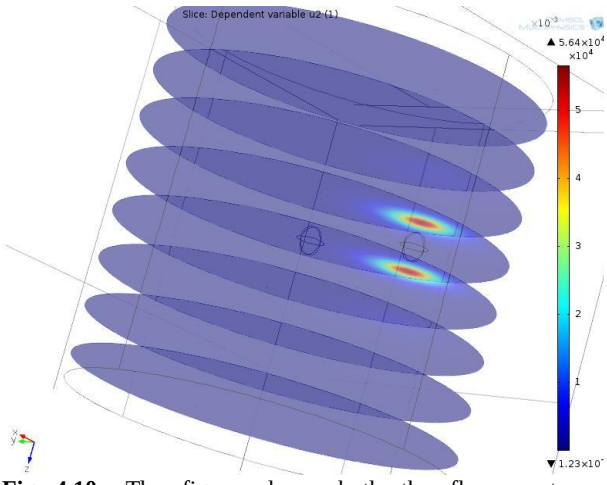

Fig 4.10: The figure shows both the fluorescent inclusions and depicts the fluorescence of the first inclusion. 8 slices were used and the simulated model here is in the xy plane.

The first fluorescent inclusion is taken at a point near to the sources as compared to the second fluorescent inclusion.

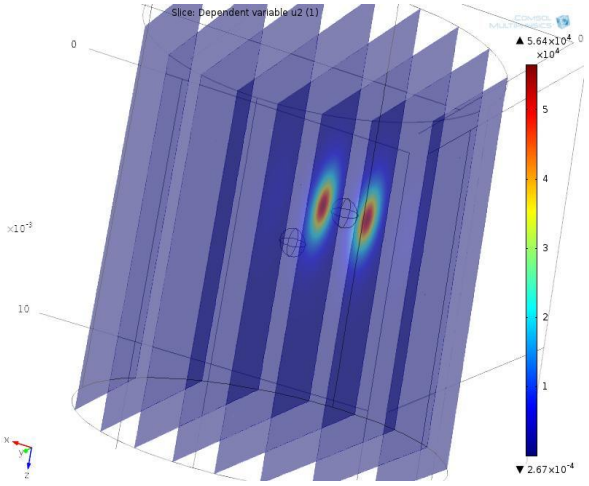

Fig 4.11 : The figure shows both the fluorescent inclusions and depicts the fluorescence of the first inclusion. 8 slices were used and the simulated model here is in the yz plane.

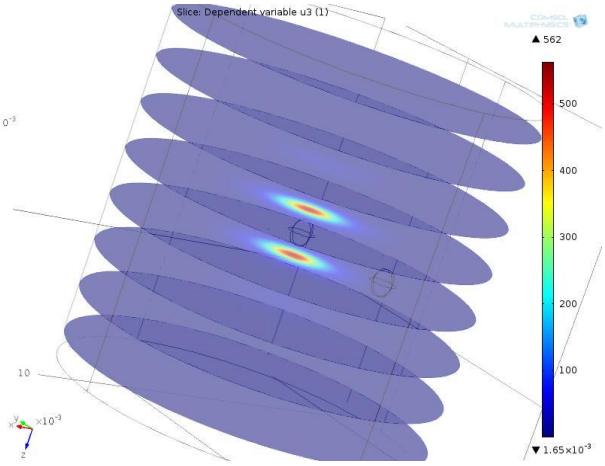

Fig 4.12 : The figure shows both the fluorescent inclusions and depicts the fluorescence of the second inclusion. 8 slices were used and the simulated model here is in the xy plane.

In visible light based medicine the fluence rate is basically the referred to as radiant exposure, which is a measurement of energy over area. The area is usually the light spot of the device.

The optical properties such as the absorption coefficient and scattering coefficient are then obtained from these fluence values.

The accuracy and precision of image reconstruction method can be evaluated by comparison between real and reconstructed values of optical properties.

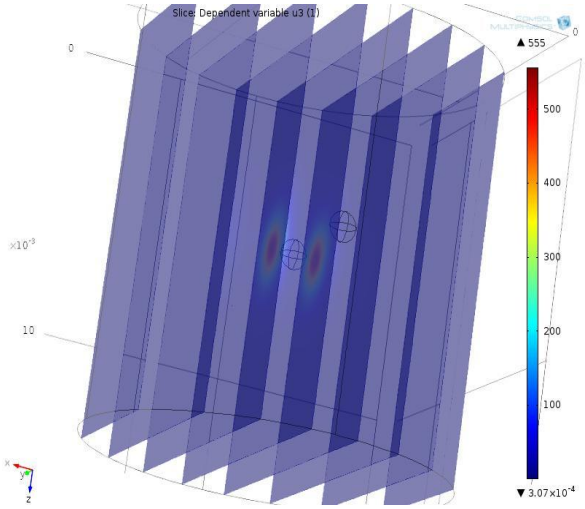

Fig 4.13 : The figure shows both the fluorescent inclusions and depicts the fluorescence of the second inclusion. 8 slices were used and the simulated model here is in the yz plane.

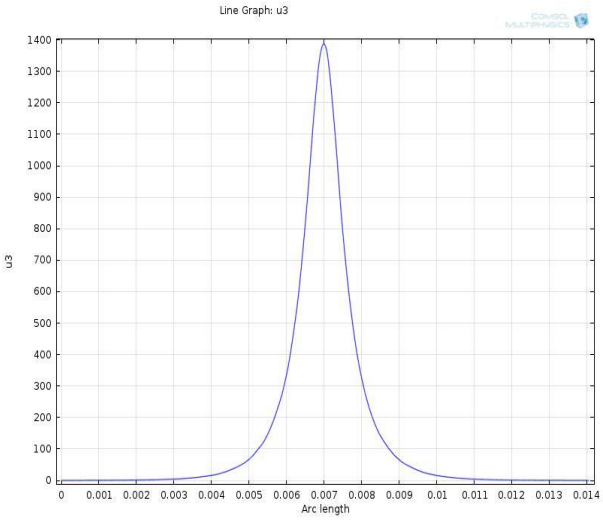

Fig 4.14: fluence rate of the second inclusion(u3) with respect to tissue thickness.

The fluence rate of the second inclusion is maximum near the inclusion and the mesh helps in obtaining these values. But when compared to the other inclusion, the measured fluence values of the second anomaly has a lesser amplitude. The amount of the fluence rate coming from the sources that is reaching the second inclusion is less as compared to the first inclusion. Therefore to increase the accuracy of the inversion, the fluence value measurement should be optimal and the type of meshing can increase the accuracy.

5.Conclusion

In this paper a 3d model of a phantom was created, which had similar properties as that of a human breast tissue. 20 sources were provided to give the required NIR radiation at the excitation wavelength (750nm) of the fluorophores. Two fluorescent inclusions were separately added and their fluorescence property observed and also a comparison was made on the fluence rate obtained.

6. Reference

1. F. Martelli, S. Del Bianco and P. Di Ninni, Perturbative forward solver software for small localized fluorophores in tissue , Biomedical optics express , vol 3 , 28-29 (2011)
2.H. Dehghani, M.E. Eames, P.K. Yalavarthy, S.C. Davis, S. Srinivasan, C.M. Carpenter, B.W. Pogue, and K.D. Paulsen, "Near infrared optical tomography using NIRFAST: Algorithm for numerical model and image reconstruction," Communications in Numerical Methods in Engineering, vol. 25, pp. 711-732,(2009)
3. Shubhadeep B, Iven J, Early detection of Breast Cancer:A molecular optical imaging approach using novel estrogen conjugate fluorescent dye, Proc.SPIE,7896, 1F8- 1F15 (2012)
3.Rebecca Richards - Kortum , Fluorescence Spectroscopy of Turbid Media.
5. Nicolas Ducros, Anabela da Silva, Jean-Marc Dinten and Françoise Peyrin, Fluorescence Diffuse Optical Tomography: A Simulation-Based Study Comparing Time-Resolved and Continuous Wave Reconstructions Performances , ISBI , 388-389(2008)
6. Albert E. Cerussi, John S. Maier, Sergio Fantini, Maria Angela Franceschini, William W. Mantulin, and Enrico Gratton, Experimental verification of a theory for the time-resolved fluorescence spectroscopy of thick tissues ,Applied Optics , Vol. 36, 116-117(1997)
7. Xiaolei Song, Ji Yi, Jing Bai, A Parallel Reconstruction scheme in Fluorescence Tomography Based on Contrast of Independent Inversed Absorption Properties, International Journal